

SYNTHESIS OF RESONANT SOUNDS WITH A HETERODYNE MODEL

Victor Lazzarini and Joseph Timoney

The Sound and Digital Music Technology Group,
National University of Ireland, Maynooth

Maynooth, Ireland

{Victor.Lazzarini,
Joseph.Timoney}@nuim.ie

ABSTRACT

This paper considers the generation of resonant waveforms from a number of perspectives. Commencing with the well-known source filter model it introduces a more advantageous heterodyne interpretation. Some variations on the basic design and comparisons with previous methods are then given. An analysis on the use of three different digital music filter structures for resonance synthesis is made, followed by an example showing how timbrally rich Frequency Modulated resonant waveforms can be synthesized.

1. INTRODUCTION

Source-modifier, also known as subtractive, synthesis is a technique whereby a complex, component-rich, source is applied to a spectrum modifier, which shapes it to produce an output matching a certain specification. In such a scenario, periodic sources are represented by oscillators and filters take the role of modifiers. This technique is perhaps the most common one found in classic analog synthesizers, and therefore is the one implemented in digital models of such instruments. Much of the literature in Virtual Analogue (VA) modelling has been concerned on how to recreate the sonic characteristics of different oscillators and filters for subtractive synthesis applications, for example see [1], [2], and [3]. A particularly musically interesting case of this technique is where the filters are capable of significantly boosting a region of their passband, close to the point of self-oscillation (where the filter becomes effectively a sinusoidal oscillator). This phenomenon is possible because the filters possess a resonance control that allows the user to adjust the filter gain in this narrow passband region only.

In addition to analog synthesizer models, there are other application scenarios where the resonant sounds play an important part. It is a well-known fact that the resonance characteristics of instruments and environments are a defining aspect of their acoustic properties [4]. In the specific case of vocal sounds, to give an obvious example, the formant characteristics of the singing voice will provide its unique timbral features [5]. These can be emulated by carefully controlled synthesis of particular resonances.

Although the most common approach to generating resonance regions in a spectrum has been to employ filters as modifiers of a component-rich input signal, there are pure signal-based alternatives. It is possible to use a variety of non-linear distortion techniques [6] to reproduce this effect. However, some of these methods, such as FM synthesis [7] and polynomial transfer-function Waveshaping ([8] and [9]) can produce unnatural variations in the spectrum in response to changes in the amount of distortion applied. As a consequence, these can be quite poor at

times in reproducing the effect of a filter. Other techniques include Summation Formulae [10], and other means of Waveshaping, [12], which will not present such issues. Additionally, specific formant resonance synthesis techniques, such as Formant Wave Synthesis (Fonction d'Onde Formatique, FOF) [13] and VOSIM [14] exist.

The case for methods of source-modifier synthesis without filters has already been successfully made in the literature [15] and here we would like to further explore the possibilities. In the following section, we will propose a technique to reproduce the typical filter-based output of resonant source-modifier synthesis by means of a heterodyne method. It offers some interesting alternatives to the typical oscillator-filter system, dispensing with the need for infinite impulse response (IIR) filters. In particular, some of these can provide accurate control of signal phases, which is problematic with IIR designs, as discussed in [16]. They also allow for efficient implementations, which are less costly than comparable methods. Following this we will analyse resonant waveform creating using other well-known musical filter structures. We will show a connection between the heterodyne model and the filter impulse response equation and use this to explore the relationship between the filter poles and the resonance signal. Lastly then, we will investigate the relationship between pole modification via modulation of the filter cutoff and the generation of a timbrally rich Frequency modulated resonant waveform. This will be achieved by example using one of these musical filters.

2. 2ND ORDER ALLPOLE RESONATORS

The general-purpose digital all-pole 2nd-order resonator filter is defined by the following equation:

$$y(n) = x(n) + 2R \cos(\omega)y(n-1) - R^2y(n-2) \quad (1)$$

where R is the pole radius ($0 \leq R < 1$), $\omega = 2\pi f/f_s$ is the pole angle (remembering that as we are dealing with real signals, there are two poles mirrored at 0Hz), f its frequency in Hz and f_s is the sampling rate. The filter centre frequency f_c (in Hz) is very close to the pole frequency f when the pole radius R is close to 1, which is the case for sharp resonances [17]. Given that we are interested in this particular case, we will assume the approximation:

$$\omega_c \approx \omega \quad (2)$$

where $\omega_c = 2\pi f_c/f_s$. For cases where this approximation is not applicable, it is possible to scale the centre frequency accordingly

(for example, a method for this is shown in [17]). The impulse response of this filter can be written as

$$s(n) = R^n \frac{\sin(\omega_c [n + 1])}{\sin(\omega_c)} \quad (3)$$

As expected, this is effectively a damped sinusoid. The amount of dampening, defined by R , will determine the resonance and bandwidth. This can be approximated (again for the case where R is close to 1, i.e. narrow bands) as:

$$R \approx \exp(-\pi \frac{f_c}{srQ}) \approx 1 - \pi \frac{f_c}{srQ} \quad (4)$$

where Q is the ratio of the filter centre frequency and its bandwidth in Hz.

2.1. Modelling a source-resonator combination

Now we have all the pieces to re-create a wideband periodic source connected to resonator as a heterodyning operation involving a sinusoidal carrier and a complex-spectrum modulator. All we need to do is to re-cast eq.3, leaving out the $1/\sin(\omega_c)$ scaling and the linear phase shift by ω_c :

$$s(n) = M(n) \sin(\omega_c n) \quad (5)$$

where $\omega_c = 2\pi f_c f_s$,

$$M(n) = R^{n \bmod T_0} \quad (6)$$

and the fundamental period $T_0 = f_s/f_0$ (with f_0 the fundamental frequency).

What we did in eq.6 was to define a periodic exponentially-decaying modulator signal (a truncated version of the infinite impulse response of eq.3). The generated signal of eq.5 will have a fundamental frequency f_0 and a resonant frequency f_c . It will produce an output that is very close to a bandlimited pulse oscillator connected to the original 2nd order all-pole filter.

A few differences are important to note, though: (i) the impulse responses will be non-overlapping and always truncated at the fundamental period length, (ii) non integral $f_c:f_0$ ratios will generate some amount of aliasing distortion (due to discontinuities at fundamental period boundaries) and (iii), generally speaking, we will also want $f_c \gg f_0$. In particular, it will not be practical to realise here the trick used to transform a resonator into a low-pass (or high-pass) filter by centring it at 0Hz (or the Nyquist). Figure 1 shows a comparison of time-domain signals generated with the heterodyne and bandlimited pulse plus filter methods, demonstrating their close similarity.

In addition to closely reproducing the magnitude effects of the filter, this algorithm also has a non-linear effect on the phases. Given that the modulator signal is an exponentially decaying signal that is periodically repeated, it will contain a mixture of sine- and cosine-phase components (plus the DC offset), which will depend on R (and T_0). This is shown by the Fourier series of the underlying continuous-time signal R^t (for $0 < t < T_0$ and with $\omega_0 = 2\pi/T_0$):

$$M(t) = \frac{R^{T_0} - 1}{T_0 \ln(R)} + \frac{2}{T_0} \sum_{k=1}^{\infty} \frac{\ln(R)(R^{T_0} - 1) \cos(k\omega_0 t) + k\omega_0(1 - R^{T_0}) \sin(k\omega_0 t)}{\ln(R)^2 + (k\omega_0)^2} \quad (7)$$

A plot of the first twenty Fourier coefficients for this signal is shown in fig.1.

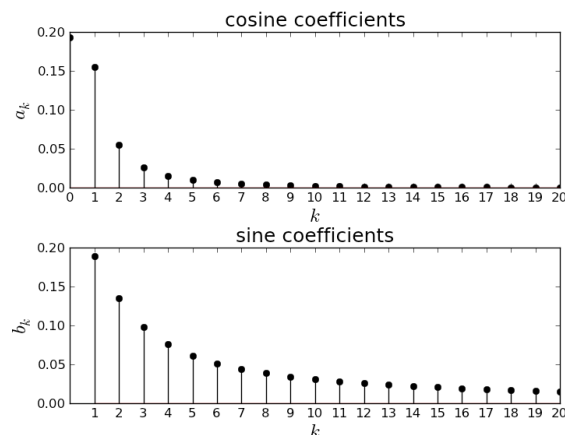


Figure 1: The first twenty Fourier series coefficients for the signal in eq.7, with $R=0.95$ and $T_0=100$.

Aliasing distortion can be problematic for high resonant frequencies, depending on the bandwidth. As noted above, such distortion can also occur if the centre frequency is not restricted to integer multiples of the fundamental. However, in general negligible amounts of aliasing were experienced if we observed these restrictions and controlled the bandwidth carefully. Note that it is also possible to dynamically change both the resonant frequency and bandwidth. To allow for smooth changes, whilst maintaining an integral $f_c:f_0$ ratio, a mix of two carriers spaced a fundamental frequency apart can be used.

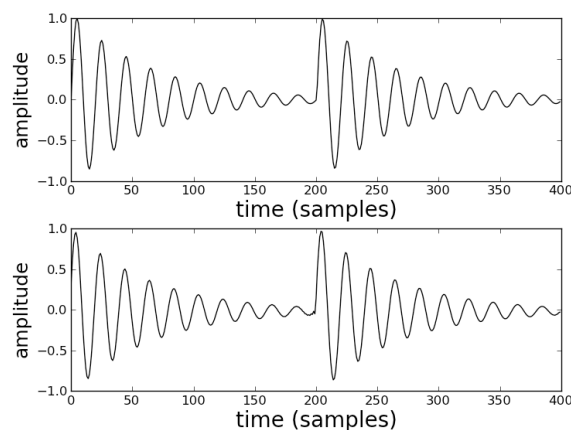


Figure 2: Comparison between resonance synthesis methods, with $f_0=220\text{Hz}$, $f_c=2200\text{Hz}$ and $Q=10$: heterodyne (top pane) and bandlimited pulse + 2nd order all-pole filter (bottom panel)

In order to vary the bandwidth of the signal, all we need to do is modify the ‘pole radius’ R dynamically. For this, we will need to find an efficient method to calculate the modulator function $M(n)$. Such a unit generator can be designed as an ‘exponential inverse phase increment’, or *eph*asor, that is, a modulo counter that accumulates an exponential quantity. Such an algorithm is shown below in a C-like code fragment:

```
eph = R;

phase = 0;
incr = f0/sr;
while(n < end){
    phase[n] += incr;
    eph[n] *= R;
    if(phase[n] > 1.0) {
        phase[n] -= 1.0;
        eph[n] = pow(R, 1+phase[n]);
    }
    n++;
}
```

This unit generator has been added to the Csound language [18] as the *eph*asor opcode, its output consisting both of the normalised phase and the exponential signal.

2.2. Fine-grained centre frequency control

Although it is possible to sweep the centre frequency of resonance in the model, leading to non-integral $f_c:f_0$ ratios, a certain amount of aliasing-induced distortion will inevitably occur. In order to allow for a better result, we will apply a method similar to the one proposed in [16]. Instead of a single carrier, we will use two, tuned to adjacent harmonics of f_0 , and we will interpolate their output, depending on the position of the real spectral peak. The revised synthesis algorithm is shown below (for positively-defined f_c and f_0 and $\omega_0 = 2\pi f_0$):

$$s(n) = M(n)[(1-a)\cos(k\omega_0 n) + a\cos([k+1]\omega_0 n)] \quad (8)$$

where

$$k = \text{int}\left(\frac{f_c}{f_0}\right) \quad (9)$$

and

$$a = \frac{f_c}{f_0} - k \quad (10)$$

This will allow us to dynamically vary the resonance frequency f_c with no additional cost to the synthesis signal quality. The same method can also be applied to the 2nd-order resonator model. This will also improve significantly its flexibility and audio quality.

3. VARIATIONS ON THE BASIC HETERODYNE RESONANCE DESIGN

The basic resonator-model design can be improved somewhat. Particularly, we note here the similarities between our approach and FOF [13] as well as VOSIM [14]. These methods share the basic idea of reproducing the filter output by concatenating a series of impulse responses in time, separated by one fundamental period.

However, there are also many differences. VOSIM is based on a series of squared sinewave pulses followed by silent gaps. The ratio between pulse bursts and silence determines the bandwidth, with longer silences widening the bandwidth. VOSIM Synthesis parameters are also substantially different from the heterodyne method, based on the number of pulses, duration of each pulse, delay gap between pulse groups, and envelope decay rate. While it might be possible to translate some of these into the heterodyne resonance method to approximate VOSIM (and vice-versa), the two techniques remain quite distinct.

FOF, however, as it is derived from a filter impulse-response perspective, is closer to our method. FOF is synthesised as a stream of grains with a set duration, possibly with two or more parallel overlapping streams if the grain durations are longer than the fundamental period. Therefore, the impulse response truncation in FOF is not linked to f_0 , as in our approach, but defined independently. For a given pole radius R , depending on how much decay we allow before truncation, a certain fundamental will imply an impulse overlap. The frequency at which this will occur at given decay in dB (dB_{decay}) and sampling rate sr is given by:

$$f_{\text{overlap}} = \frac{20 \times \ln(R)sr}{\ln(10)\text{dB}_{\text{decay}}} \quad (11)$$

Nevertheless, with a carrier tuned to a multiple of the fundamental frequency, the question of overlapping or non-overlapping impulses becomes one of scaling. This is because the overlapped sections are guaranteed to be in-phase, and if the overlap is significant, there will be a comparative increase in the output gain in relation to the non-overlapping case. This is enough to justify our simpler approach, characterised by just a multiplication of two signals, which is, therefore, more computationally efficient. In fact, its overall cost is comparable to its equivalent filter implementation, whereas FOF can be much more costly.

From FOF, however, we can borrow the principle of shaping the start of the impulse response, thereby improving the slope of the system’s magnitude response. By employing a second modulator, tuned to the same fundamental, but with a much wider bandwidth (therefore a shorter effective duration) and subtracting it from the first modulator, we can reproduce the effect:

$$s(n) = (M_a(n) - M_b(n))\sin(\omega_c) \quad (12)$$

The resulting signal will approximate very closely the effect of FOF synthesis at a reduced computational load. A plot of a waveform generated using this method is shown in fig. 3, where it is compared to an equivalent FOF waveform. Disregarding some minor phase differences, the two waveforms are reasonably similar.

3.1. Resonant Wave synthesis

Similarities with other techniques also exist. Most notably, we see a close connection with the ‘resonant wave’ method implemented in the Casio CZ series of synthesisers [19]. In it, the carrier-modulator arrangement is also present, but in a much less controlled and formal set-up. According to the original patent [20], the modulator signal is produced by an inverted modulo counter (phasor), ie. a non-bandlimited sawtooth wave ,

$$saw(n) = 0.5 + 0.5 \sum_{k=1}^{\infty} \frac{1}{k} \sin(k\omega_0 n) \quad (13)$$

with $\omega_0 = 2\pi f_0$, producing an output defined by

$$saw(n) \sin(\omega_c n) = 0.5 \sin(\omega_c n) + 0.25 \sum_{k=1}^{\infty} \frac{1}{k} [\cos(\omega_c n - k\omega_0 n) - \cos(\omega_c n + k\omega_0 n)] \quad (14)$$

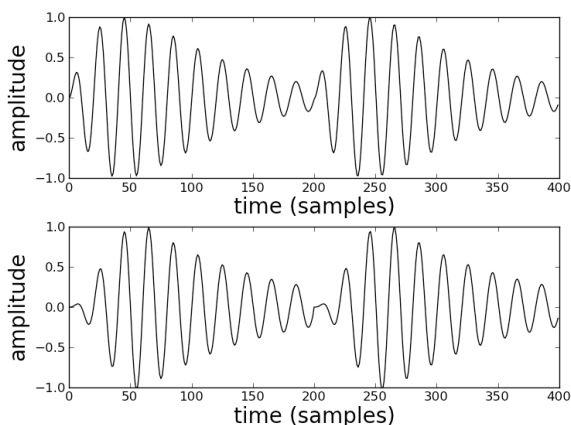


Figure 3: A FOF-like resonant waveform generated using a heterodyne method (upper panel) and an equivalent waveform generated by the original FOF algorithm (lower panel).

While we will get a resonant region around f_c , we will not have any means of effectively controlling its bandwidth, as we do with the resonator model. In addition, aliasing distortion might become an issue as eq.13 is non-bandlimited. A quick examination of eq.12 will lead us to conclude that the resonance bandwidth will depend on the fundamental frequency. Here, lower fundamentals will produce narrower bandwidths. In terms of its phase spectrum, we observe here a more stable pattern, whereby components above the centre frequency will exhibit an offset of π radians in relation to the ones in the lower side. As expected, sweeping the resonance frequency will also lead to some amount of perceptible aliasing distortion, which is not ideal.

The Casio implementation allows for two other modulator shapes: a triangle and a trapezoid, which will provide different resonance bandwidths. However, it does not provide any means of dynamically changing one shape into the other. One way around this would possibly be arranged with the addition of some means of interpolation between two or more shapes stored in function tables. The modulator shape will have a significant impact on the resulting signal, given that it is its spectrum that determines the magnitude response of the equivalent filter we are trying to model.

3.2. Implementation

A single phase generator, or modulo counter, is used to synchronise the phases of the modulator and carrier signals. The sinusoids are implemented using table lookup. Thus, for the heterodyne realisation of source-modifier synthesis with a resonator model, we have three unit generators: an ephasor and two table

readers. The former implements the exponentially decaying modulator described earlier. It produces two output signals, a normalised phase (between 0 and 1) and a decaying exponential. Its inputs are the ‘pole radius’ R and the fundamental frequency f_0 . The two table readers take in a normalised phase and generate the double carrier signal, tuned to integral multiples of the fundamental. The output is scaled by the amplitude A . A block diagram of this method is shown on Figure 4.

4. OTHER MUSICAL FILTERS: SECOND ORDER POLE/ZERO COMBINATIONS AND HIGHER ORDERS

The principles given in Sections 2 and 3 can be applied for the analysis of musical filters that are associated with subtractive synthesis [21]. These are intimately associated with resonant waveforms as mentioned in the introduction. However, these musical filter structures are more complicated than the original 2nd order all-pole system employed in the first sections of this paper. It is advantageous though to see how the results so far can be generalised; particularly the relationship between the value of the Pole and the shape of the Modulator waveform. Furthermore, they can be used as a stepping stone from which other musically interesting phenomenon such as Filter-based Frequency Modulation synthesis can be explored.

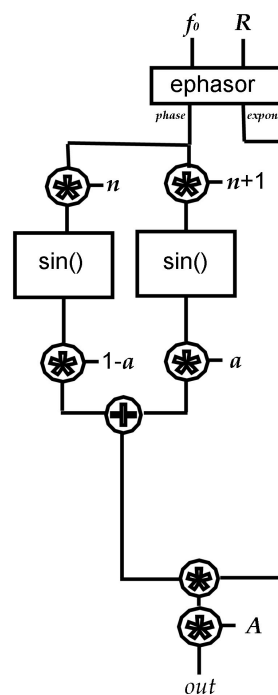


Figure 4 Heterodyne Resonator synthesis block diagram

To begin with, we will write the equation for the impulse response of a resonant 2nd order pole-zero filter in terms of its poles and zeros. We will then give the equations for well-known second order music filters: the Sallen Key [22], associated with Korg MS-20 [23], and the State variable filter [24], associated with Oberheim [25]. Next, we will consider a simple 4th order filter with feedback used to create a resonance [26]. We will show how the pole trajectories for these filters influence the properties of the resonant waveform. Then, we will consider an example of how modulation of the filter cutoff frequency when the filter resonance is at its peak creates a timbrally rich frequency modulated signal.

4.1. Second order pole-zero filters

If we have the transfer function of a general second-order digital filter

$$H(z) = \frac{b_0 + b_1 z^{-1} + b_2 z^{-2}}{1 + a_1 z^{-1} + a_2 z^{-2}} \quad (15)$$

This filter will have an impulse response [27]

$$h(n) = -\left(\frac{b_2}{a_2}\right) + r_1(P_1)^n + r_2(P_2)^n \quad (16)$$

where $n=0,1,2,\dots$, P_1 and P_2 are the poles of the transfer function, and the residues r_k ($k=1,2$) are given by

$$r_k = H(z)(1 - P_k z^{-1})_{z=P_k} \quad (17)$$

If the poles are complex conjugates of each other, as is required for resonant behaviour, then

$$P_1 = P_2^* \quad (18)$$

and

$$r_1 = r_2^* \quad (19)$$

where the asterisk denotes the complex conjugate

Thus the expression for the impulse response can be rewritten

$$h(n) = -\left(\frac{b_2}{a_2}\right) + r_1(P_1)^n + r_1^*(P_1^*)^n \quad (20)$$

or in Polar form

$$h(n) = -\left(\frac{b_2}{a_2}\right) + |r_1|e^{j\angle r_1} (|P_1|e^{j\angle P_1})^n + |r_1|e^{-j\angle r_1} (|P_1|e^{-j\angle P_1})^n \quad (21)$$

Rearranging gives

$$h(n) = -\left(\frac{b_2}{a_2}\right) + 2|r_1||P_1|^n \cos(n\angle P_1 + \angle r_1) \quad (22)$$

Thus, in general the 2nd order impulse response of a system with poles and zeros is comprised of

- (1) a DC term: $-(b_2/a_2)$
- (2) a cosine of frequency: $\angle P_1$ and phase shift: $\angle r_1$
- (3) a decaying exponential: $|P_1|^n$
- (4) a magnitude term: $2|r_1|$

Returning to eq. 22 we can see that the modulator term is equivalent to

$$M(n) = 2|r_1||P_1|^n \quad (23)$$

Lastly, for all IIR filters the poles can be computed from the well-known formula for quadratics [27]

$$P_{1,2} = \frac{-a_1 \pm \sqrt{a_1^2 - 4a_2}}{2} \quad (24)$$

and the residue r_1 will be

$$r_1 = \frac{b_0 + (b_1/P_1) + (b_2/P_1^2)}{(1 - (P_2/P_1))} \quad (25)$$

4.2. 2nd Order musical filters: Digital Sallen Key Filter

The feedforward coefficients for a digital Sallen Key Filter are [22]

$$\begin{aligned} b_0 &= 1/(1 + 2\zeta C + C^2) \\ b_1 &= 2b_0 \\ b_2 &= b_0 \end{aligned} \quad (26)$$

and the feedback coefficients are

$$\begin{aligned} a_1 &= 2(1 - C^2)/(1 + 2\zeta C + C^2) \\ a_2 &= (1 - 2\zeta C + C^2)/(1 + 2\zeta C + C^2) \end{aligned} \quad (27)$$

where ζ is a damping parameter (inverse of resonance) and

$$C = 1/\tan(0.5\omega_c) \quad (28)$$

where ω_c is the cutoff frequency.

4.3. 2nd Order musical filters: Digital State Variable Filter

The digital state variable filter has feedforward coefficients [24]

$$\begin{aligned} b_0 &= b_2 = 0 \\ b_1 &= F^2 \end{aligned} \quad (29)$$

and feedback coefficients

$$\begin{aligned} a_1 &= F^2 + DF - 2 \\ a_2 &= 1 - DF \end{aligned} \quad (30)$$

where

$$D = \min\{\zeta, 2 - \omega_c/\pi\} \quad (31)$$

and

$$F = (\omega_c/\pi)(1.85 - 0.85D(\omega_c/\pi)) \quad (32)$$

4.4. 4th order filter with resonance

The 4th order lowpass filter is another very common musical filter. It consists of four single-order sections connected in cascade, giving a 24dB/octave roll-off [26]. However, to obtain resonant 'corner peaking' a regenerative path is included. The transfer function of a single digital section for a normalised sampling frequency is given by [29]

$$H_1(z) = \frac{(1/3)(1+z^{-1})}{1-(1/3)z^{-1}} \quad (33)$$

with the overall structure of the 4th order system as shown in fig.5, where g is the gain of the feedback path

The gain g for this filter varies between 1 and 4 [26]. This filter is referred to as a ‘polygon filter’ which reflects the trajectory of the poles in the complex plane as the value for g is varied, that is they lie at the corners of a 4-sided polygon [28]. The impulse response for this system can be written in a form that is similar to eq. 22

$$h(n) \approx 2|r_1||P_1|^n \cos(n\angle P_1 + \angle r) + 2|r_3||P_3|^n \cos(n\angle P_3 + \angle r_3) \quad (34)$$

where any DC term has been omitted for convenience. In the case of a resonant waveform output from the filter then $P_1 \gg P_3$ and the second component of eq.34 will decay almost instantaneously in comparison to the first.

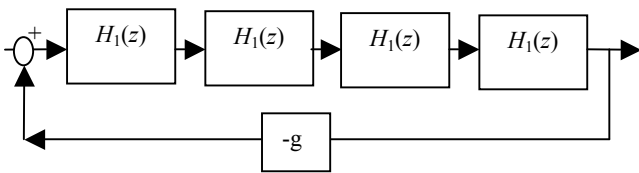


Figure 5: Block diagram of 4th order musical filter with feedback path for resonance

4.5. Analysis

Figure 6 shows the trajectory of the poles on the unit circle of the three different musical filters for a fixed cutoff frequency of 441Hz and the resonance parameter varying from 0 to 100%. The top panel is for the Sallen Key Filter, the middle panel for the State Variable filter and the bottom panel for the 4th order filter.

From figure 6 it can be seen that the Poles of the Sallen Key filter trace out a parabolic shape from 1 to 0.94 on the real axis, while those of the State Variable filter are almost straight from 1 to 0.98. Those of the 4th order filter have a diagonal path, the polygon shape, from 1 to 0.94 and 0.88 to 0.94. Referring to eq. 21 these trajectories highlight how the decay of the modulator component of the resonance waveform varies with respect to the resonance, as this is dependent on the absolute value of the pole. Figure 7 illustrates this for the three filters. Here, poles values from the minimum to maximum values are taken and their exponential decay is plotted for $n=0$ to 8192 samples. Normalisation is applied for comparison purposes.

In the figure it can be seen that as the pole value increases from its smallest value to its maximum, the slope of the decay changes. However, in both the case of the Sallen Key and State Variable filters the maximum value must be very close to unity as the decay is very long. Furthermore, there is a noticeable difference between the decay for the maximum and of the other pole values, particularly for the Sallen Key filter. However, for the 4th order filter there appears a better balance in the decay as the pole value increases. This appears to be well-behaved and suggests it would respond in a more perceptually pleasing manner to a steady incremental control.

4.6. Frequency modulated filter cutoff

Awareness of the relationship between the filter cutoff and the pole value also allows the consideration of the effect of modulating the filter cutoff on the resonance waveform. This effect is known in Subtractive synthesis as Filter FM (Frequency Modulation) or Audio Mod and is associated with the Sequential Circuits Prophet synthesizers and the more modern DSI instruments [30]. The filter should be at full resonance. Without any modulation this will produce a pure, or approximate, sinewave output. Modulation of the filter cutoff though will produce a nonlinear frequency modulation.

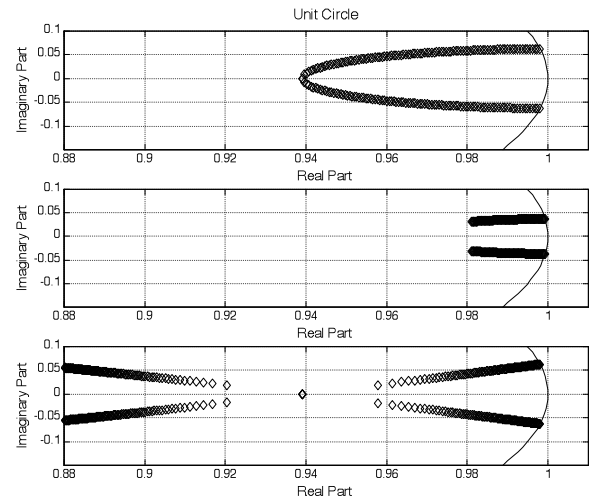


Figure 6: Unit circle pole trajectories as a function of resonance for the Sallen Key (top panel), State variable (middle panel) and 4th order (bottom panel) filters.

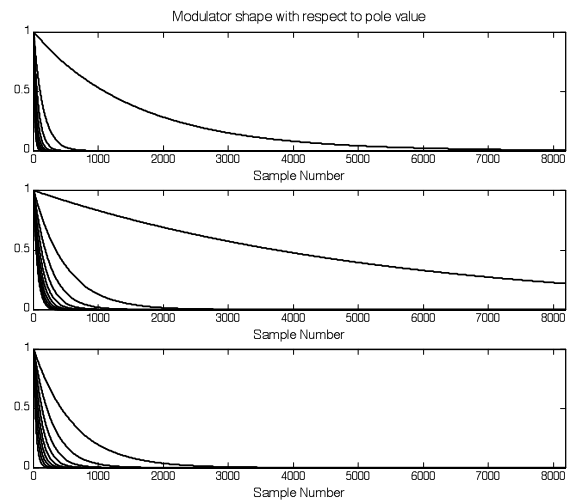


Figure 7: variation in the modulator shape with respect to the pole value for the Sallen key (top panel), State variable (middle panel), and 4th order (bottom panel) filters.

This can be seen for example by examining the equations for the Sallen Key filter. Here, $\zeta=0$ for full resonance. This means that

$$b_0 = \frac{1}{1+C^2} \quad (35)$$

The equation for the pole is given by

$$P_1 = -b_0(1-C^2) + \sqrt{(b_0(1-C^2))^2 - b_0(1+C^2)} \quad (36)$$

Substituting eq. 35 into eq. 36 and after some manipulation an equation for the pole can be approximated as

$$P_1 = 1 + j \frac{2 \tan(\omega_c/2)}{1 + \tan^2(\omega_c/2)} \quad (37)$$

This results in an approximation for the pole angle

$$\angle \hat{P}_1 = \tan^{-1} \left(\frac{4\omega_c}{4 + \omega_c^2} \right) \quad (38)$$

This can be substituted into an equation of the form of eq. 22 but where sample index n varies periodically with period f_0 , and the magnitude of the pole is unity, $|P_1| = 1$, to give the FM resonant waveform

$$q(n) = 2|r_1| \cos((n \bmod f_0) \angle \hat{P}_1 + \angle r_1) \quad (39)$$

If the cutoff frequency then is time varying at audio rate according to some desired shape such as a sinusoid or triangle wave then the pole angle in eq. 39 will be time varying giving

$$q_{fm}(n) = 2|r_1| \cos((n \bmod f_0) \angle \hat{P}_1(n) + \angle r_1) \quad (40)$$

Figure 8 plots an example of an FM resonant wave. The top panel is a sinusoidal modulation of the filter cutoff between 1Hz and the cutoff of 441Hz. The modulation depth is thus 440Hz. Furthermore, the modulation rate is 441Hz. The middle panel shows the instantaneous frequency of the resonant waveform found by differencing the phase angle of eq. 40. The frequency f_0 is the same as the cutoff. This has the effect of bringing the envelope of the resonant waveform to zero at the start of every new period, and thus causes large negative spikes in the instantaneous frequency. The instantaneous frequency is a smooth function, resulting in the FM resonant waveform in the bottom panel. Figure 9 plots the spectrum of this FM resonant waveform, and because the frequencies of the modulator and cutoff modulation are the same, the signal has a purely harmonic spectrum, with new harmonics appearing above the modulation frequency of 441Hz.

Figure 10 shows the spectrum of a different example, using the same cutoff modulation shown in Figure 8, but where the period of the modulator waveform, and so n , is set as 735Hz. Thus, there is a non-integer relationship between this and the cutoff modulation frequency. Here, many harmonic and inharmonic components are visible, related to the cutoff modulation frequency and f_0 . This spectrum appears to be very timbrally rich and the inharmonicity present in this FM signal suggests that it is good for the production of bell-like and metallic sounds [30].

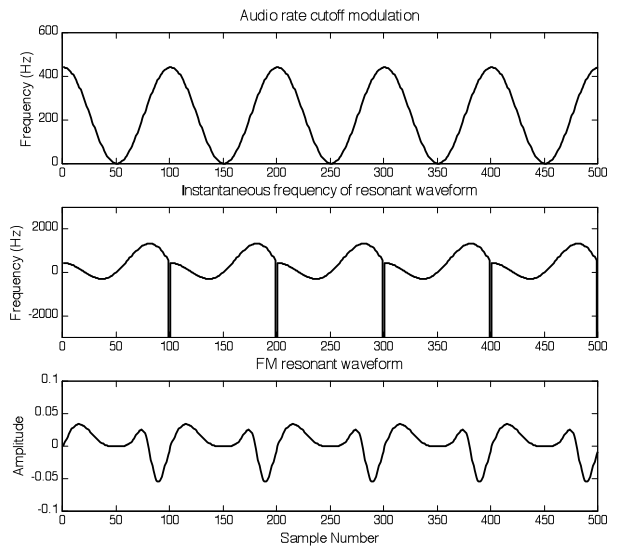


Figure 8: Example of FM resonant waveform: Audio rate cutoff modulation (Top panel), Instantaneous Frequency of Resonant Waveform (Middle panel) and FM Resonant waveform (Bottom panel)

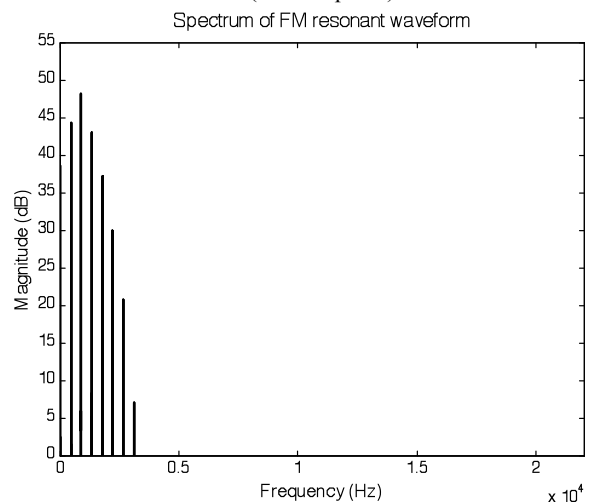


Figure 9: Spectrum of the FM resonant waveform example. The length of the FFT was 2^{16} and a Hanning window was used.

A similar approach can be taken to create a Frequency modulated resonant waveform outputs from the other musical filter structures. More theoretical analysis would be required to give a definitive evaluation on the quality of the FM resonant waveforms created. This requires the waveform modulation to be described in terms of a set of individual, spectrally convolved modulators in order to discern the effect of each one, as outlined by the procedure given in [31].

5. CONCLUSIONS

This paper proposed a heterodyne approach for the synthesis of resonant waveforms. Methods for fine-tuning the frequency control and a computationally efficient design were explained. Analysis of three different digital music filters for resonance synthesis was carried out and the 4th order 'polygon' filter appeared to

have the steadiest relationship between the degree of resonance, pole magnitude, and modulator decay. Modulation of the filter cutoff frequency was shown to produce a timbrally rich Frequency Modulated resonant waveform with harmonic and inharmonic components whose presence depends on the relationship between the cutoff modulation, f_c , and the modulator frequency, f_0 .

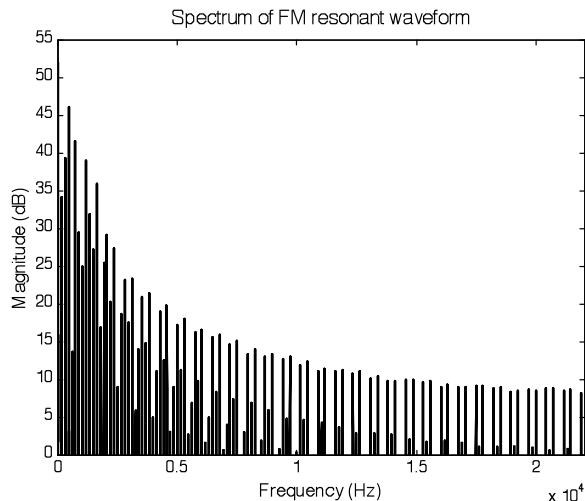


Figure 10: Spectrum of the inharmonic FM resonant waveform example. The length of the FFT was 2^{16} and a Hanning window was used.

Future work will expand the analytical contribution by further investigating the relationship between the musicality of a filter and its pole trajectories with respect to the size of the resonance parameter. It will also attempt to formalize the spectral properties of the FM resonant waveform so that its control using the filter cutoff modulator parameters can be better understood.

6. REFERENCES

- [1] J. Lane, D. Hoory, E. Martinez and P. Wang, 'Modeling Analog Synthesis with DSPs', *Computer Music Journal* 21(4), 1997, pp. 23-41.
- [2] V. Välimäki and A. Huovilainen, 'Oscillator and Filter Algorithms for Virtual Analog Synthesis', *Computer Music Journal* 30(2), 2006, pp.19-31.
- [3] V. Lazzarini, and J. Timoney, "New Perspectives on Distortion Synthesis for Virtual Analog Oscillators", *Computer Music Journal* 34(1), 2010, pp.28-40.
- [4] J. Backus, *The Acoustical Foundations of Music*, Norton, 2nd Ed., New York, 1977.
- [5] D. Howard and J. Angus, *Acoustics and Psychoacoustics*, Focal Press, 4th Ed., London, 2009.
- [6] C. Dodge and T. Jerse, *Computer Music*, Schirmer Books, New York, NY, 1985.
- [7] J. Chowning, 'The Synthesis of Complex Audio Spectra by Means of Frequency Modulation', *Journal of the Audio Engineering Society* (21), 1973, pp. 526-34.
- [8] D. Arfib, 'Digital Synthesis of Complex Spectra by Means of Multiplication of Non-Linear Distorted Sinewaves', *AES Preprint No.1319* (C2), 1978.
- [9] M. LeBrun, 'Digital Waveshaping Synthesis', *Journal of the Audio Engineering Society* 27(4), 1979, pp. 250-266.
- [10] G. Windham and K. Steiglitz, 'Input Generators for Digital Sound Synthesis', *Journal of the Acoustic Society of America*, 47(2), 1970, pp. 665-6.
- [11] J. A. Moorer, 'The Synthesis of Complex Audio Spectra by Means of Discrete Summation Formulas', *Journal of the Audio Engineering Society*, 24 (9), 1976, pp.717-727.
- [12] J. Timoney, V. Lazzarini and T. Lysaght 2008, 'A modified FM synthesis approach to bandlimited signal generation', *Proceedings of the International Conference on Digital Audio Effects*, Helsinki, Finland, 2008, pp.27-33.
- [13] X. Rodet, 'Time-Domain Formant-Wave Function Synthesis', *Computer Music Journal* 8(3), 1984, pp. 9-14.
- [14] W. Kaegi and S. Tempelaars, 'VOSIM-A New Sound Synthesis System', *Journal of the Audio Engineering Society*, 26(6), 1978, pp. 418-425.
- [15] J. Lazzaro, and J. Wawrzynek, 'Subtractive Synthesis without Filters,' *Audio Anecdotes*, K. Greenebaum, (ed), A. K. Peters Ltd., Natick, MA, 2003.
- [16] M. Puckette, 'Formant-Based Audio Synthesis Using Nonlinear Distortion,' *Journal of the Audio Engineering Society* 43(1), pp.40-47, 1995.
- [17] K. Steiglitz, *Digital Signal Processing Primer*, Prentice-Hall, Englewood Cliffs, NJ, 1996.
- [18] R. Boulanger (Ed.), *The Csound Book*, MIT Press, Cambridge, Mass., 2000.
- [19] H. Massey, A. Noyes and D. Shklair, *A synthesist's guide to acoustic instruments*, Amsco publications, New York, NY, 1987.
- [20] M. Ishibashi, 'Electronic Musical Instrument', *U.S. Patent no. 4,658,691*, 1987
- [21] M. Russ, *Sound synthesis and sampling*, Focal press, Elsevier, Oxford, UK, 2009.
- [22] U. Zölzer (ed), *DAFX: digital audio effects*, John Wiley and sons, Chichester, UK, 2002.
- [23] T. Stinchcombe, A study of the Korg Ms-10 and MS-20 filters, 2006.
www.timstinchcombe.co.uk/synth/MS20_study.pdf
- [24] J. Dattorro, 'Effect Design, Part 1: Reverberator and Other Filters,' *Journal of the Audio Eng. Soc.*, 45(9), Sept. 1997, pp. 660-684.
- [25] CEM3320 Filter Designs, *Oberheim OB-Xa 2-pole Lowpass Filter*, 2012.
<http://www.electricdruid.net/index.php?page=info.cem3320>
- [26] B. Hutchins, 'Additional design ideas for voltage-controlled filters', *Electronotes*, vol. 10, 85(5), Jan. 1978.
- [27] J. McClellan, R. Schaffer, and M. Yoder, *DSP first: a multimedia approach*, Prentice Hall, US, 1998.
- [28] R. Bjorkman, 'A brief note on polygon filters', *Electronotes*, vol. 11, 97(7), Jan. 1979.
- [29] T. Stilson, and J. Smith, 'Analyzing the Moog VCF with Considerations for Digital Implementation', *Proc. Int. Comp. Music Conf.*, San Fransisco, USA, 1996, pp. 398-401.
- [30] Dave Smith Instruments, *Prophet 08 manual*, 2012, www.dsisynt.com/KM1107.DaveSmith.pdf
- [31] J. Timoney and V. Lazzarini, 'A homomorphic interpretation of the complex FM expansion', *AES 45th International Conference on Applications of Time-Frequency Processing in Audio*, Espoo, Finland, Mar. 2012.